Wave *RUN-UP* Measurements under very oblique wave incidence

Análise do espraiamento sob estados de agitação de incidência oblíqua

Rute LEMOS[1], Vera PINA[2], João Alfredo SANTOS[2,3], Conceição FORTES[1], Maria Teresa REIS[1], Antje BORNSCHEIN[4]

[1] LNEC - Laboratório Nacional de Engenharia Civil, Av. do Brasil, 101, Lisboa, rlemos@lnec.pt, jfortes@lnec.pt, treis@lnec.pt

[2] ISEL – Instituto Superior de Engenharia de Lisboa, Instituto Politécnico de Lisboa, Rua do Conselheiro Emídio Navarro, 1, Lisboa, A41697@alunos.isel.pt, jasantos@dec.isel.ipl.pt

[3] CENTEC – Centre for Marine Technology and Ocean Engineering, Universidade de Lisboa, Av. Rovisco Pais, Lisboa

[4] TU Dresden - Technische Universität Dresden, antje.bornschein@tu-dresden.de

ABSTRACT: Under the scope of the HYDRALAB+ transnational access project, the so-called RODBreak experiment was conducted in the multidirectional wave basin at the Marienwerden facilities of the Leibniz University Hannover (LUH). A stretch of a rubble-mound breakwater was built in the wave basin with a very gentle slope. Its armour layer was made of Antifer cubes, at the roundhead and adjoining trunk, and of rock, at the rest of the trunk.

A set of tests was carried out to extend the range of wave steepness values analysed in wave run-up, overtopping and armour layer stability studies, focusing on oblique extreme wave conditions, with incident wave angles from 40º to 90º.

The present study focuses on the analysis of measured wave run-up values obtained in the tests and on their on their variability as well as the influence of the wave obliquity and directional spreading.

Keywords: rubble-mound breakwaters; run-up; oblique waves; physical modelling; RODbreak.

RESUMO: No âmbito do projeto RODBreak (projeto de Transnational Access do projeto HYDRALAB+), foram realizados ensaios no tanque de ondas multidirecionais das instalações de Marienwerden da Leibniz University Hannover (LUH).

Foi construído, no tanque de ondas irregulares, um troço de um quebra-mar de taludes de inclinação suave. O seu manto resistente era constituído por cubos Antifer na zona da cabeça e tronco adjacente, e por pedra, no resto do tronco. Foi realizado um conjunto de testes de modo a alargar o leque de valores de declividade das ondas na análise do espraiamento, galgamento e estabilidade do manto resistente, com ênfase em condições agitação extremas e com obliquidade variando entre 40º e 90º. O presente estudo centra-se na análise dos valores de espraiamento obtidos durante os ensaios e na sua variabilidade, bem como na influência da obliquidade da onda e da dispersão direcional.

Palavras-chave: Quebra-mares de talude; espraiamento, obliquidade; modelação física.

Este artigo é parte integrante da *Revista Recursos Hídricos*, Vol. 42, N.º 1, 81-90 março de 2021.

1. INTRODUCTION

Most climate scenarios predict the sea-level rise, as well as increased intensity and frequency of storms (IPCC, 2014). Wave breaking / run-up / overtopping and their impact on the stability of rubble-mound breakwaters (both at trunk and roundhead) are not adequately characterized yet for climate change scenarios. The same happens with the influence oblique wave attack on such phenomena, especially for angles over 45°.

To ensure an adequate performance of these coastal structures in such scenarios without having to increase the size of the breakwaters and the associated costs, it is mandatory to understand the influence of the wave attack angle, as well as the effect of the directional spreading on their response in what concerns wave run-up, wave overtopping and armour layer stability.

In particular, wave run-up characteristics on coastal structures are crucial for predicting the occurrence of overtopping, for studying coastal flooding and/or for evaluating the impact of this phenomenon on people's safety, on the integrity of goods and infrastructure, and on the normal performance of economic activities at the areas protected by these structures.

Several former investigations on wave run-up and overtopping of impermeable and permeable coastal structures aimed at quantifying the influence of oblique waves on mean overtopping discharge, water layer thickness and velocities through the development of empirical formulas for a reduction factor, $\gamma\beta$ (Nørgaard *et al.*, 2013). However, most of the formulas did not consider very oblique wave approach.

According to the European Overtopping Manual, EurOtop (Van der Meer *et al.*, 2018), the angle of wave attack β is the angle at the toe of the structure, after any transformation on the foreshore by refraction or diffraction, between the direction of the waves and the perpendicular to the longitudinal axis of the structure. There it is stated that, for incidence angles larger than 45°, the wave overtopping will eventually become zero.

Only limited research is available on the influence of oblique wave attack on wave run-up and wave overtopping due to the complexity and the high costs of model testing in wave basins. Most of the relevant research was performed in flumes and consequently on the influence of long crested waves. Only few investigations are available on the influence of short-crested waves.

One of these investigations aiming to fill the gap on the effect of oblique waves on the run-up and overtopping, was the experimental work of Pohl *et al.*, 2014 and Bornschein *et al,* 2014, under the framework of HYDRALAB-project CornerDike, to study the influence of a curved-axis dike on the spatial distribution of wave run-up and wave overtopping.

The main goal of that experimental work was to adjust the prediction formulas, which seem to fairly converge with measured overtopping for small incidence angles only. In fact, for tested incidence angles between 0 and 112.5º, the wave run-up and overtopping do decrease with increasing angles of incidence but, did not become zero as predicted.

On the other hand, the influence of the corner curved axis was also studied, revealing that the distance from the corner of the dike and the subsequent influence of diffraction at the corner do contribute to a decrease of the overtopping.

Despite these advances on wave run-up and overtopping characterization and predicting formulae for impermeable slopes, some gaps remain in what concerns the characterization of these phenomena on rough, permeable slopes, as well as the study of the influence of the roundhead on them.

The existing data gaps triggered the RODBreak experiment, whose main goal is to contribute to a better understanding of the wave run-up, overtopping and damage in rubble-mound breakwaters, under extreme wave conditions, including different obliquity and directional spreading.

Under extreme wave conditions (wave steepness of 0.055) with different incident wave angles (from 40° to 90°), a total of 49 tests were performed in the wave basin of LUH, where a stretch of a rubble-mound breakwater was implemented. For each test, several measurements were carried out, including run-up measurements with five capacitive wave probes 0.87 m long, that were placed along the model slope, 3 at the breakwater trunk and 2 at the breakwater roundhead.

The objective of the present work is to analyse, for a rough permeable slope under the action of sea-waves with a steepness of 0.055, the run-up heights obtained in the tests and their variation with wave obliquity and directional spreading (long and short-crested waves).

2. PHYSICAL MODEL, INSTRUMENTATION AND WAVE CONDITIONS

A stretch of a rubble mound breakwater (head and part of the adjoining trunk, with a slope of 1(V):2(H)) was built in the wave basin of the LUH to assess, under

extreme wave conditions (wave steepness of 0.055) with different incident wave angles (from 40º to 90º), the structure behaviour in what concerns wave run-up, wave overtopping and damage progression of the armour layer. Two types of armour elements (rock and Antifer cubes) were tested. The trunk of the breakwater is 7.5 m long and the head has the same cross section as the exposed part of breakwater. The total model length is 9.0 m, the model height is 0.82 m and its width is 3.0 m.

Figure 1 presents the physical model as well as a profile with detailed model dimensions.

Test series comprised long and short crested waves. Two water depths of 0.60 m and 0.68 m and five incidence wave angles (40º, 55º, 65º, 75º and 90º) were considered for long crested waves, while for short crested waves only one water depth (0.60 m) was considered and 2 incident wave angles (40º and 65º), with a directional spreading of 50º. Given one water depth and one incident direction, each daily test sequence consisted of at least 4 tests for different wave conditions acting on the model (Hs = 0.100 m, 0.150 m, 0.175 m and 0.200 m and the corresponding peak periods Tp = 1.19 s, 1.45 s, 1.57 s and 1.68 s). A total of 52 tests were made.

Table 1 summarizes the test parameters of the four-test sequences analyzed in the present paper, where d is the water depth, H_{m0} is the spectral significant wave height, T_p is the spectral peak period, all measured in front of the wave generator. β is the angle of wave attack and σ is the directional spreading width.

Incident and reflected sea waves were measured with three arrays made of six acoustic wave gauges (Array 3.1, 3.2 and 3.3).

A wave gauge array (array 3.3) was deployed in front of the wave maker, another in front of the breakwater head, (array 3.2) aligned with the breakwater crest, and one approximately at the middle of the breakwater trunk (array 3.1) in front of the entrance to the second overtopping reservoir.

In front of the entrance to the first and third overtopping reservoirs, two isolated acoustic wave gauges (G1.1.1 and G1.1.3) were deployed. A third acoustic wave gauge was deployed in front the breakwater head (gauge G1.1.3).

Overtopping reservoirs with weighing cells were used to measure the water volume that overtopped a stretch of the crest of the breakwater. That water then fell into the reservoir, and its volume could then be measured with the weighing cells. Water-level gauges were also installed in the overtopping reservoirs for redundancy in the measurement of the overtopping volume.

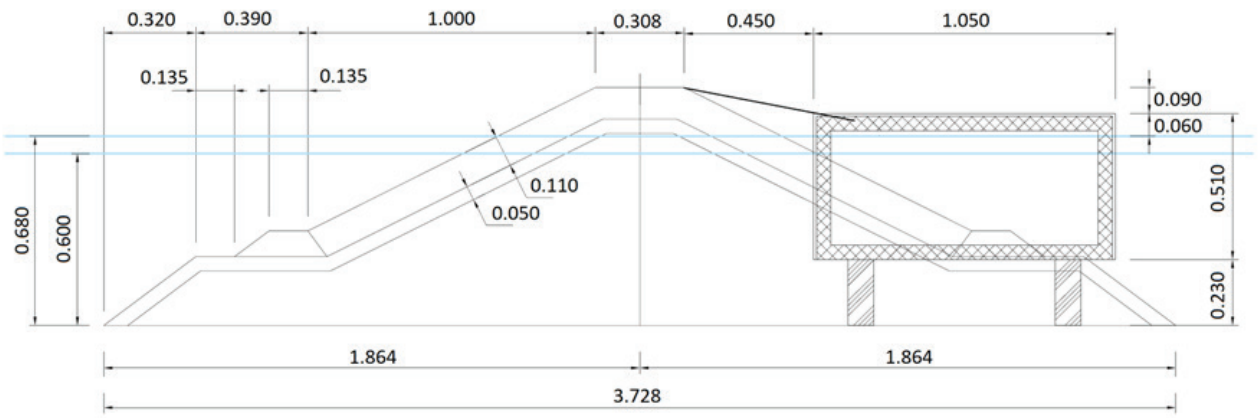

Figure 1. Breakwater model.

Table 1. Test parameters.

Test	d (m)	Hm0 (m)	Tp (s)	β (°)	σ (°)
13	0.60	0.100	1.19	40	0
14		0.150	1.45		
15		0.175	1.57		
16		0.200	1.68		
17	0.60	0.100	1.19	65	0
18		0.150	1.45		
19		0.175	1.57		
20		0.200	1.68		
21	0.60	0.100	1.19	90	0
22		0.150	1.45		
23		0.175	1.57		
24		0.200	1.68		
25		0.250	1.88		
27	0.68	0.100	1.19	40	0
28		0.150	1.45		
29		0.175	1.57		
30		0.200	1.68		
31	0.68	0.100	1.19	65	0
32		0.150	1.45		
33		0.175	1.57		
34		0.200	1.68		
35	0.60	0.100	1.19	40	50
36		0.150	1.45		
37		0.175	1.57		
38		0.200	1.68		
39		0.250	1.88		
40	0.60	0.100	1.19	65	50
41		0.150	1.45		
42		0.175	1.57		
43		0.200	1.68		
44		0.250	1.88		
45	0.60	0.100	1.19	55	0
46		0.150	1.45		
47		0.175	1.57		
48		0.200	1.68		
49	0.60	0.100	1.19	75	0
50		0.150	1.45		
51		0.175	1.57		
52		0.200	1.68		
58	0.68	0.100	1.19	55	0
59		0.150	1.45		
60		0.175	1.57		
61		0.200	1.68		
63		0.250	1.88		
64	0.68	0.100	1.19	40	50
65		0.150	1.45		
66		0.175	1.57		
67		0.200	1.68		
68		0.250	1.88		

To measure the wave run-up, five capacitive wave gauges (G4.1.1, G4.1.2, G4.1.3, G4.1.4 and G4.1.5) were deployed on the armour layer of the breakwater trunk and head. Note that the armour layer where G4.1.1 and G4.1.2 (trunk) are located is made of rock units, while G4.1.4 and G4.1.5 are located on the head of the breakwater, with an armour layer made by regularly placed Antifer cubes. The same is valid for the G4.1.3 gauge which is located at the trunk stretch whose armour layer made of Antifer cubes.

An alternative to measure the run-up consisted in a chequered staff on the slope of the breakwater trunk. By analysing the frames of the video recorded with a camera over the staff, the length of the staff wetted by each wave can be measured, hence the run-up estimated.

Figure 2 presents the plan view of the breakwater model, as well as the different equipment categories, according to the variables measured: sea waves; run-up and overtopping.

The present work focuses on the wave run-up height measurements using the capacitive wave gauges.

3. RESULTS

To analyse the wave run-up along the breakwater, the wave gauges data from G4.1.2 and G4.1.4 were analysed. Those wave gauges were chosen since they are located at the trunk and the head of the breakwater, respectively. To characterize the wave parameters (H_{m0} and $T_{m-1,0}$) in front of those wave gauges, a spectral analysis was conducted (Spans *et al.*, 2019) based on the data from arrays 3.1 and 3.2 located on the vicinity of wave run-up gauges G4.1.2 and G4.1.4, respectively (see Fig. 2).

The wave run-up height is defined as the vertical difference between the highest point of wave run-up and the still water level (SWL). To obtain the wave run-up, a temporal analysis was carried out in the time series of the free surface elevation measured at each test at the wave gauges G4.1.2 and G4.1.4 (located at middle of the trunk and at the head of the breakwater, perpendicularly to the breakwater crest).

The angle between the wave gauge and the armour layer slope was considered following the procedure presented in Götz (2019). Extreme values found in some measurements, mainly caused by water splashes, were removed in order to prevent those values to be considered as maximum run-up and possibly causing calculation distortions. The MatLab algorithm for run-up computation enable to visualize the corrected run-up time series.

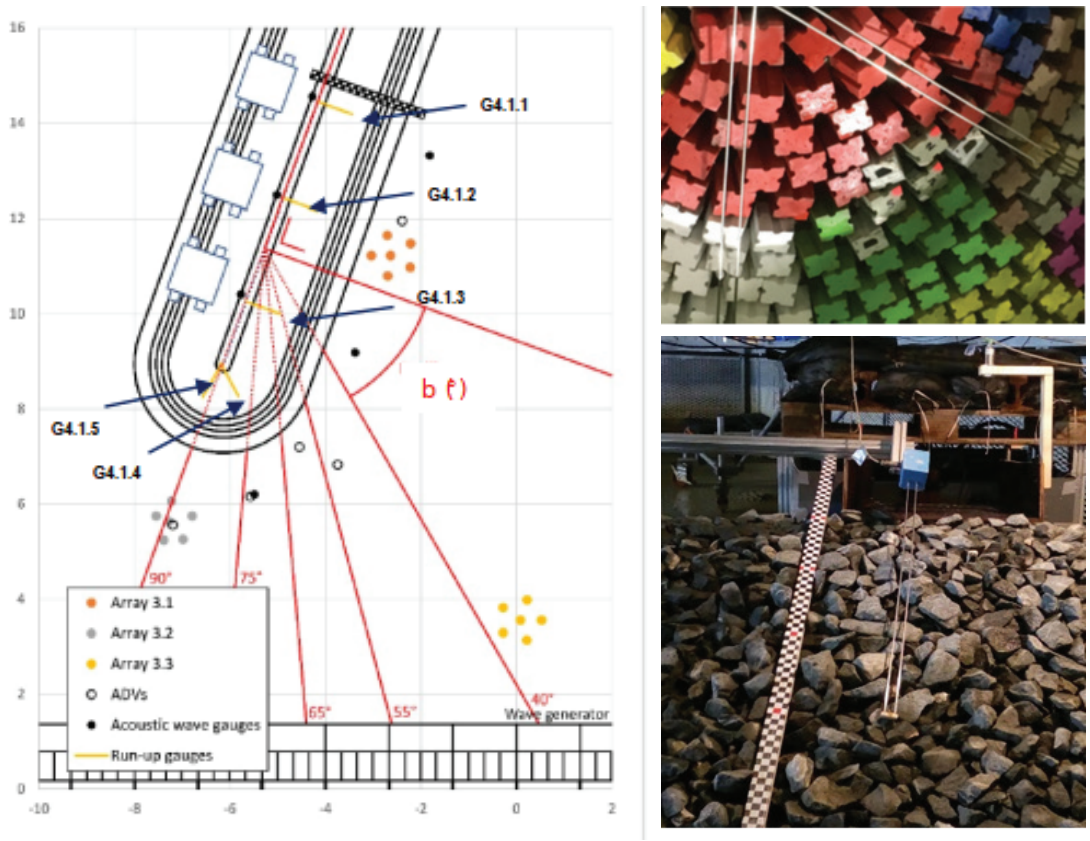

Figure 2. Plan view of the model and equipment and wave directions.

From the ordered series of run-up values for a given incident sea state, it was determined $Ru_{2\%}$, which is the wave run-up level that is exceeded by 2% of the incoming waves. Ru_{max} (the maximum run-up height) and Ru_{med} (the average run-up height) were also calculated.

In the present work, the data analysis is focused on the 2% run-up height, as it is considered a good quantity for the design of dike height. If only 2% of run-up waves of the sea state reach the crest of the breakwater, potentially inducing overtopping, this number of waves is considered so small that no special measures have to be taken to strengthen this part of the breakwater.

The analysis made aimed to evaluate, for wave gauges G4.1.2 and G4.1.4, the influence of the angle of wave attack and of the directional spreading on the wave run-up height. The results obtained on those different sections of the breakwater, provided some insights on how the distance from the head of the breakwater can contribute for the wave run-up decrease.

4.1 Variability of the relative run-up

Figure 3 presents, for gauges 4.1.2 and 4.1.4, the relative run-up, given by $Ru_{2\%}/Hm0$ as a function of the breaker parameter. This dimensionless run-up parameter $Ru_{2\%}/Hm0$ enables to compare the $Ru_{2\%}$ for different conditions, regardless the significant wave height, Hm0. The breaker parameter, also known as surf similarity or Iribarren number is defined as $\xi m\text{-}1,0 = \tan\alpha/(Hm0/L_{m\text{-}1,0})½$, where α is the slope of the front face of the structure and $L_{m\text{-}1,0}$ being the deep water wave length $gT^2_{m\text{-}1,0}/(2\pi)$. The breaker parameter $\xi_{m\text{-}1,0}$ permits to infer on the trend of run-up height for various wave periods.

The results are presented for the five different wave angles of attack with long-crested waves, as well as with short-crested waves for the angles of attack of β =40° and β =65°.

According to Figure 3, the breaker parameter values are between 2.25 and 3.03, for G 4.1.2 and between 2.16 and 2.46 for G4.1.4, which is mostly according to the theory presented in EurOtop, where, for rubble-mound breakwaters, with steep slopes (1:1.5 or 1:2), the range of the breaker parameter ($\xi_{m\text{-}1,0}$) is often between 2 and 4.

In the present study, for the proposed wave steepness (0.055) and slope angle ($\tan\alpha$=0.5), the breaker parameter was expected to be around 2.13. Nevertheless, the breaker parameter presented some spread, mainly due to the wave transformation caused by the structure. The standard deviation for G.4.1.4 was of 0.076, while for G.4.1.2 was of 0.16, mostly due to tests conducted with β =90°, whose breaker parameter ranged between 2.61 and 3.03.

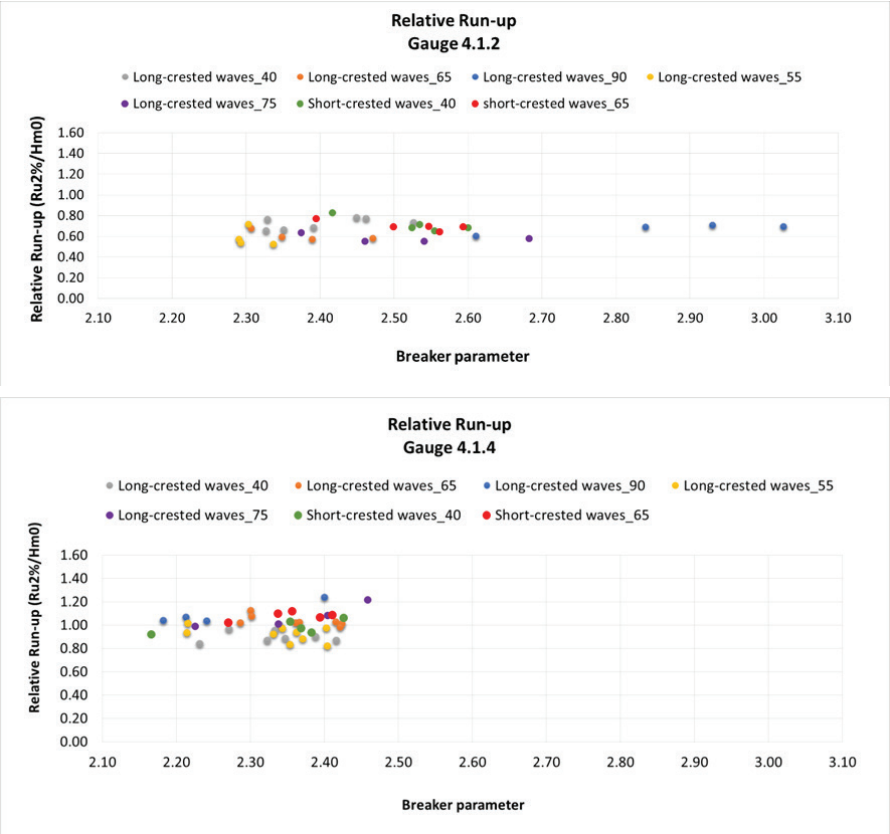

Figure 3. Relative run-up for G 4.1.2 and G 4.1.4.

The influence of the head of the breakwater may have contributed to this higher standard deviation. In what concerns the relative run-up values, for G4.1.2, at the trunk, the values are between 0.53 and 0.82 whereas at the head, gauge G4.1.4, they are between 0.82 and 1.3. Relative run-up heights at G4.1.2 were significantly lower than in G4.1.4. This can be caused by the different type of armour units (rock or Antifer cubes) and the influence of the head of the breakwater. A rock armour slope dissipates significantly more energy than a regularly placed Antifer armour, as the roughness of the armour layer can decrease the wave run-up height. The influence of the distance from the breakwater´s head on the wave transformation can also justify the decrease of relative run-up.

It was also noticeable that relative run-up values obtained at G4.1.2 for the test series conducted with $\beta = 90^{\circ}$ and $\beta = 75^{\circ}$ are of the same order (average of 0.63) and presented low variability with a standard deviation of 0.06.

Figure 4 presents the comparison between tests conducted with long-crested waves (test series T13-T16 and T17T20) and short-crested waves (test series T35-T39 and T40-T44). For both gauges, results obtained in tests with short-crested waves (hollow markers) presented less variability than in tests with long-crested waves.

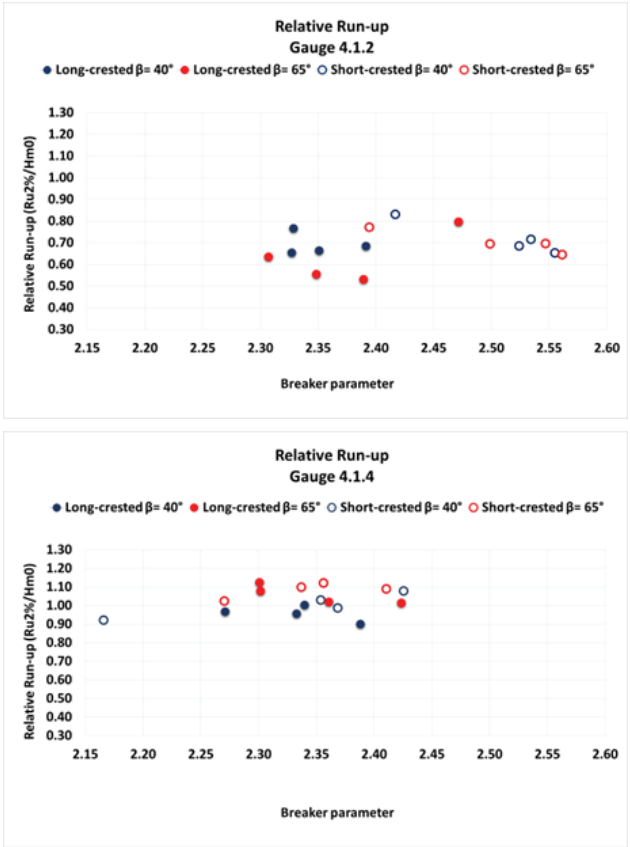

Figure 4. Comparison between tests conducted with long and short-crested waves. Relative run-up for G 4.1.2 and G 4.1.4.

4.2 Influence of the spreading width

In the following figures, the relative run-up is compared, for tests conducted with angles of wave attack of 40° and 65° and spreading widths of 0° and 50°. Values above the line means that the relative run-up is larger for spreading width 50°. Values below the line means that the relative run-up is larger for spreading width 0°. Table 2 presents, for both wave gauges and for wave angle attack of 40° and 65°, the average relative run-up absolute differences between spreading widths of 0° and 50°. According to the results presented in Figure 5, tests with spreading width of 50° present higher relative run-up than with 0° (most of the markers are above the line). For G4.1.2 this trend is more noticeable for β =65° than with β=40°.

For wave gauge G4.1.4, the difference was not so expressive (half of the markers are above the line and the other half are below), probably due to the diffraction around the head of the breakwater.

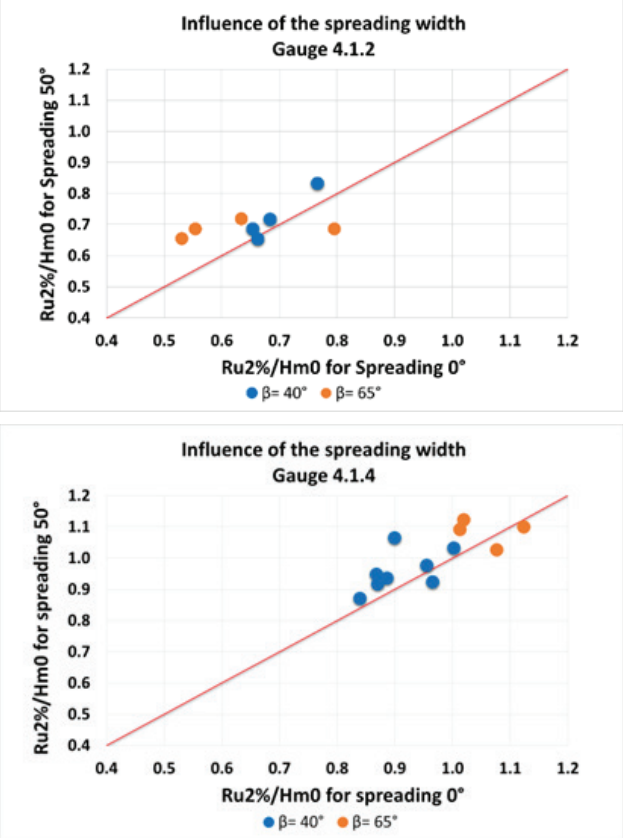

Figure 5. Influence of the spreading width on $Ru_{2\%}$ for G 4.1.2 and G 4.1.4.

Table 2. Average relative run-up differences between spreading widths of 0° and 50°

Angle of attack (°)	Relative Run-up average differences between spreading widths 0° and 50°	
	G4.1.2	G4.1.4
40	0.053	0.057
65	0.084	0.047

4.1.2 Influence of the angle of attack

In this section, aiming to infer on the influence of the angle of attack on the run-up height, one proceeds to a similar analysis as for the influence of the spreading width, but in this case, values of relative run-up obtained with the angle of attack β=40° are compared with the values obtained with angles associated with an higher obliquity, β=55°, β=65°, β=75°and β=90° (Figure 6 and Figure 7). Table 3 presents, for both wave gauges, the average relative run-up absolute differences between angles of attack.

Regarding G4.1.2, Figure 6, one can observe that relative run-up decreases for higher angles of attack (most of the markers are below the line) except for 90°. Once again, the diffraction on the head of the breakwater may have influence on those results.

For short-crested waves the angle of wave attack seems to have less influence. This is mainly caused by the fact that within the wave field, there are individual waves whose directions are different from the main direction β.

Regarding G4.1.4, Figure 7, it can be observed that relative run-up increases for higher angles of attack. As for G4.1.2., one can find lower differences between tests conducted with short-crested waves.

Table 3. Average relative run-up differences between angles of attack for wave gauges G4.1.2 and G4.1.4.

Angles	Relative Run-up average differences	
	G4.1.2	G4.1.2
β =40° vs β=55° long-crested waves	0.138	0.047
β =40° vs β =65° long-crested waves	0.152	0.124
β =40° vs β =65° short-crested waves	0.022	0.081
β =40° vs β =75° long-crested waves	0.108	0.120
β =40° vs β =90° long-crested waves	0.064	0.138

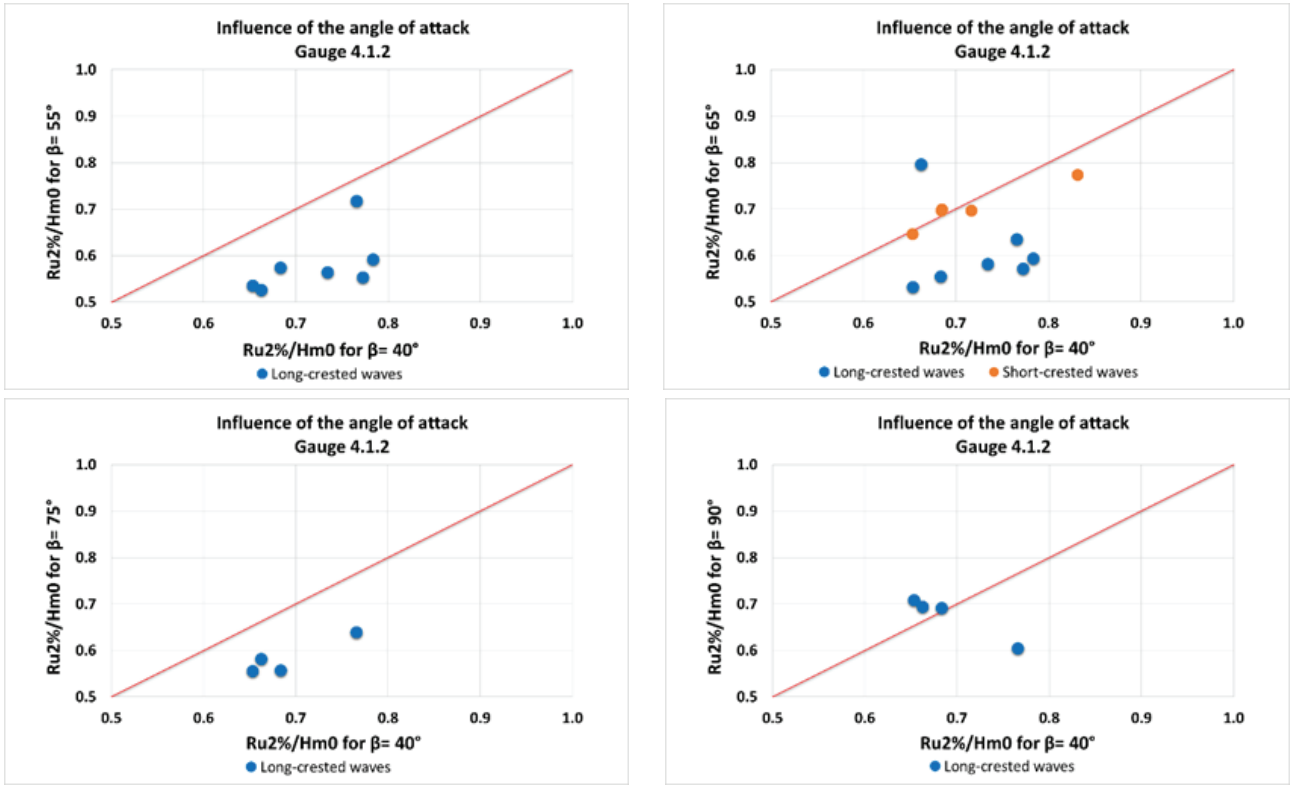

Figure 6. Influence of the angle of attack on Ru2% for G 4.1.2

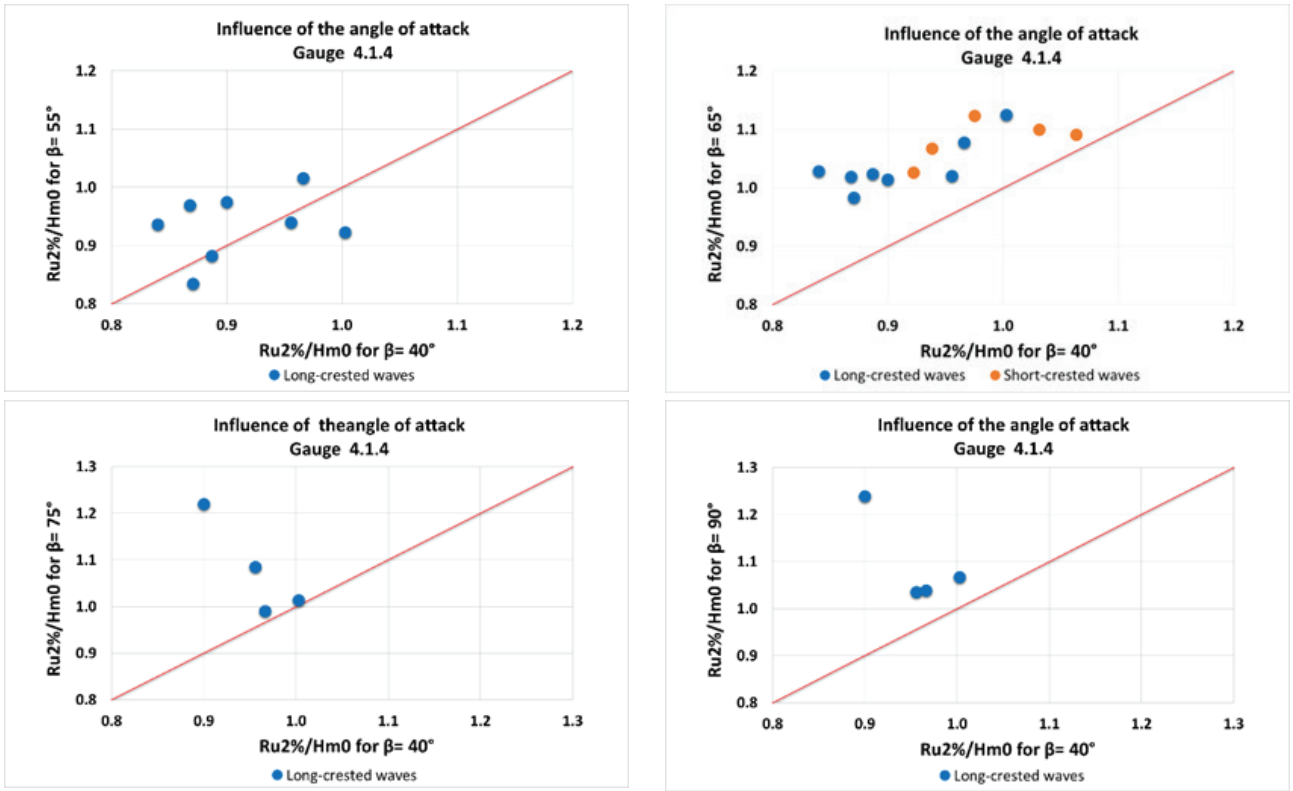

Figure 7. Influence of the angle of attack on Ru2% for G4.1.4.

4. DISCUSSION

The presented study was based upon a set of tests conducted with oblique extreme wave conditions, with incident wave attack angles ranging between 40º and 90º, with long and short-crested waves.
This paper focused on the analysis of the measured wave run-up values obtained during those tests and on their variability, as well as the influence of the wave obliquity and directional spreading. The conclusions arisen from the analysed data are:

- In what concerns the **relative run-up variability**, in the present study, for the proposed wave steepness (0.055) and slope angle (tanα=0.5), the breaker parameter was expected to be around 2.13. The spread of the breaker parameter on both gauges lead to higher standard deviation at G.4.1.2, mostly due to tests conducted with β =90º (The influence of the head of the breakwater may have contributed to this higher standard deviation).

  The relative run-up at G4.1.2 was significantly lower than in G4.1.4. This can be explained both due to the influence of the head of the breakwater and because of the type of armour units. A rock armour slope dissipates significantly more energy than a regularly placed Antifer armour, as the roughness of the armour layer can decrease the wave run-up height.

  The influence of the distance from the breakwater´s head on the wave transformation can also justify the decrease of relative run-up and should be investigated. For both wave gauges, results obtained in tests with short-crested waves (hollow markers) presented, in a general way, less variability than in tests with long-crested waves.

- Regarding the **influence of the spreading width**, in a general way, tests with spreading width of 50° present higher relative run-up than with 0°. At the trunk (G4.1.2) this trend is more noticeable for tests with β=65º than with β=40º. This is in agreement with the results presented by Oosterlo (2013) in a report following the Cornerdike project where, for the higher angles of incidence, a higher overtopping was found when the incident sea waves had large spreading widths.

  At the roundhead (G.4.1.4), the difference was not so expressive, probably due to the wave transformation at the head of the breakwater.

- Regarding the **influence of the angle of attack**, it was observed that in the breakwater trunk (G4.1.2), relative run-up decreases for higher angles of attack except for 90°. The influence of the head of the breakwater on those results should be investigated in a more detailed study. Results at G4.1.4 (roundhead) revealed that relative run-up increased for higher angles of attack.

  For both wave gauges, in tests with short-crested waves the angle of wave attack seems to have less influence. This is mainly caused by the fact that within a wave field, there are individual waves whose directions are different from the main direction β, and consequently diminishing the importance of the angle of attack.

- Future work will comprise the analysis of wave gauges G4.1.1 and G4.13 located at the trunk, in order to infer on the variability of the wave run-up with the distance from the head of the breakwater and with different armour layer roughness.

ACKNOWLEDGMENTS

This project has received funding from the H2020 research and innovation programme under grant agreement No 654110, HYDRALAB+. The project To-SEAlert, Ref. PTDC/EAM-OCE/31207/2017 and BSafe4Sea, Ref. PTDC/ECI-ECG/31090/2017 are also acknowledged.

REFERENCES

Bornschein, A., Pohl, R., Wolf, V., Schüttrumpf, H., Scheres, B., Troch, P., Riha, J., Spano, M., Van der Meer, J. (2014). Wave run-up and wave overtopping under very oblique wave attack (CORNERDIKE-project). Proc. HYDRALAB IV Joint User Meeting, Lisbon, July.

Götz, M. (2019). Wave Run-Up at Mole Structures. Master Thesis, Technische Universitat Dresden.

IPCC, Climate change (2014). Synthesis report. Contribution of working groups I, II and III, in: R.K. Pachauri, L.A. Meyer (Eds.), Fifth Assessment Report of the Inter. Panel on Climate Change, IPCC, Geneva, 2014

J.Q.H. Nørgaard, T. Lykke Andersen, H.F. Burcharth, G.J. Steendam (2013). Analysis of overtopping flow on sea dikes in oblique and short-crested waves, Coast. Eng. 76, 43–54.

Oosterlo, Patrick. (2013). Influence of very oblique waves on wave overtopping. Bachelor thesis, TUDelft, doi: 10.13140/RG.2.1.2685.7847.

Pohl, R., Bornschein, A. u. a. (2014): Effect of very oblique Waves on Wave Run-Up and Wave

Overtopping, CORNERDIKE (HYIV-DHI-05). Dresdner Wasserbauliche Mitteilungen; Heft 52, ISBN 978-3-86780-392-2

Spans, J.H.; Santos, J.A.; Fortes, C.J.E.M.; Pinheiro, L., 2019 - Analysis of the incident sea-waves and of the consequent run-up in the RODBreak experiment. SCACR2019, 9-11 de setembro, Bari, Itália. 152-157pp ISBN 978-88-97181-73-6. Editora: EdiBios.

Van der Meer, J.W., Allsop, N.W.H., Bruce, T., De Rouck, J., Kortenhaus, A., Pullen, T., Schüttrumpf, H., Troch, P. and Zanuttigh, B. EurOtop (2018). Manual on Wave Overtopping of Sea Defences and Related Structures. An Overtopping Manual Largely Based on European Research, but for Worldwide Application, www.overtopping-manual.com